Suppressed "Warburg Effect" in Nasopharyngeal Carcinoma Via the Inhibition of Pyruvate Kinase Type M2-Mediated Energy Generation Pathway

Penglong Zhao, MBBS[1], Mengyan Zhou, MMed[1],
Ruixiang Chen, MBBS[1], and Renjie Su, MMed[1]

Abstract

Warburg effect describes the abnormal energy metabolism in cancer cells and pyruvate kinase type M2 is involved in the regulation of this effect. In the current study, the role of pyruvate kinase type M2 in the initiation of Warburg effect in nasopharyngeal carcinoma cells was explored. The expression status of pyruvate kinase type M2 was detected in nasopharyngeal carcinoma samples and analyzed by different clinicopathological characteristics. Then the level of pyruvate kinase type M2 was suppressed in 2 nasopharyngeal carcinoma cell lines. The effects of pyruvate kinase type M2 inhibition on cell viability, apoptosis, invasion, glucose uptake, ATP generation, and glycolysis metabolism were determined. The data showed that the high expression of pyruvate kinase type M2 in nasopharyngeal carcinoma tissues was associated with the larger tumor size and advanced metastasis in the patients. The inhibition of pyruvate kinase type M2 resulted in the repressed proliferation and invasion in nasopharyngeal carcinoma cells, along with the increased apoptotic rate. The lack of pyruvate kinase type M2 function inhibited glucose uptake, while increased ATP generation in nasopharyngeal carcinoma cells. Moreover, the production of glycolysis metabolites, including pyruvic acid, lactate, citrate, and malate, was also suppressed by pyruvate kinase type M2 inhibition. At molecular level, the expressions of glucose transporter and hexokinase 2 were downregulated by pyruvate kinase type M2 inhibition, confirming the changes in glucose metabolism. Collectively, the current study demonstrated that the function of pyruvate kinase type M2 was important to maintain the proliferation and invasion of nasopharyngeal carcinoma cells, and the inhibition of the factor would antagonize nasopharyngeal carcinoma by blocking Warburg effect.

Keywords

Abbreviations

Introduction

Nasopharyngeal carcinoma (NPC) is a type of malignancy derived from the nasopharyngeal mucosal lining.[1] Based on previous investigations conducted in 2016, NPC was recognized as one of the most common malignancies in South East Asia and southern China.[2] Over the last decades, the management strategies for NPC have been developed by liquid

[1] Department of Otolaryngology-Head and Neck Surgery, The First People's Hospital of Wenling, Wenling, Zhejiang Province, China

Corresponding Author:
Renjie Su, Department of Otolaryngology-Head and Neck Surgery, The First People's Hospital of Wenling, No. 333 Chuan'an South Road, Chengxi Street, Wenling 317500, Zhejiang Province, China.
Email: rj_su_wl1976@outlook.com

biopsies, minimally invasive surgery, and advanced chemotherapeutic and immunotherapeutic methods.[3] However, the prognosis of patients with NPC is rendered less satisfactory for those with locally advanced and metastatic tumors.[4,5] Therefore, the identification of novel and sensitive biomarkers associated with NPC progression is of critical importance. This will also improve the development of handling methods based on these biomarkers.

The majority of mammalian cells in adulthood are in the quiescent phase. The cells utilize the available nutrients as an energy source for the majority of their functions. However, this biological process is disturbed in cancer cells, which utilize nutrients for energy production and macromolecular biosynthesis. The latter is used to support the abnormal cell growth and DNA replication of cancers.[6] During this process, higher uptake of glucose and increased rates of glycolysis and production of lactate are observed even under aerobic conditions. This phenomenon is defined as the "Warburg effect" according to the name of the scientist who discovered it.[7] Numerous cancer types, including NPC,[8,9] converge on this metabolic pathway to meet their energetic demands during their progression.[6] Therefore, in recent years, the suppression of the Warburg effect has been proposed as a promising strategy to control cancers arising from different types of cells. For example, the inhibition of long noncoding RNA LINC00504 contributes to decreased aerobic glycolysis and reduces the progression of ovarian cancer.[10] The induction of miR-150-5p expression inhibits the Warburg effect and consequently proliferation, migration, and invasion of melanoma cells.[11] With regard to NPC, knockdown of STYK1 and JMJD2A contributes to the control of NPC via the suppression of the Warburg effect.[8,9] Nevertheless, although substantial efforts have been made to uncover the pathways associated with the initiation of the Warburg effect, the detailed mechanism underlying this biological process remains unclear. It is of great interest to further explore the factors associated with the development of the Warburg effect, which will not only explain the oncogenesis of different cell types but will also provide novel cancer therapeutic methods for certain types of cancers including NPC.

In addition to the aforementioned mechanisms, the studies by Christofk *et al* have demonstrated that the development of the Warburg effect is regulated by the activity of the glycolytic enzyme pyruvate kinase (PK). More specifically, it has been reported that the enzyme pyruvate kinase M2 (PKM2) enables cancer cells to utilize aerobic glycolysis instead of oxidative phosphorylation.[12,13] Pyruvate kinase M2 is a specific alternative splice isoform of PK that catalyzes the final step of glycolysis. It is well-characterized that the expression of PKM2 is advantageous over the other PK isoforms for cancer cell growth since inhibition of PK allows the transformation of glycolytic intermediates in the pentose phosphate pathway.[14,15] For instance, the switch of PK expression from PKM2 to the constitutively active M1 isoform results in reduced cell proliferation and a decreased ability to form solid tumors.[12,16] Moreover, the inhibition of PKM2 suppresses tumor growth and invasion in lung carcinoma and osteosarcoma.[17,18] Despite

the close interaction between PKM2 and the Warburg effect that has been verified in multiple cancer types, its function in NPC has not been previously explored. Therefore, in the current study, the expression levels of PKM2 in NPC specimens were investigated. In addition, the association between PKM2 expression and clinicopathological features of patients with NPC was explored. The expression of PKM2 was also inhibited in NPC cell lines; and the effects on cell proliferation, cell mobility, and metabolic factor activity were assessed. The present study provides valuable information for elucidating the mechanism by which PKM2 influences the progression of NPC and aims to facilitate the development of PKM2-targeted strategies for the treatment of this disease.

Materials and Methods

Patients and Tumor Specimen Collection

A total of 44 pairs of NPC and corresponding glioma tissues were collected between 2015 and 2016 at The First People's Hospital of Wenling. All the patients were diagnosed with NPC and their detailed clinicopathological characteristics were collected. All patients provided a written informed consent form for their participation in the study. The patients who had received radiotherapy or chemotherapy were excluded from the database.

Cell Culture and Detection of PKM2 Expression Status

The human nasopharyngeal epithelial cell line NP69 and the NPC cell lines CNE2, CNE1, HNE1, 5-8F, and 6-10B were purchased from Jennio-bio (Guangzhou, China). The NP69 cells were cultured in keratinocyte/serum-free medium (Invitrogen) at 37 °C in an atmosphere of 5% CO_2 and 95% air. All the NPC cell lines were cultured in Roswell Park Memorial Institute-1640 medium (Gibco) supplemented with 10% fetal bovine serum (HyClone) at 37 °C in an atmosphere of 5% CO_2 and 95% air. The expression levels of PKM2 in the cell lines were detected using reverse transcription-quantitative PCR (RT-qPCR) and Western blot assays. The activity of PKM2 was detected using ELISA Kit for PKM2 according to the manufacturer instruction (IBL).

Quantitative Real-Time Polymerase Chain Reaction

Total RNA was extracted using the RNA Purified Total RNA Extraction Kit according to the manufacturer instructions (BioTekea). Subsequently, the RNA was incubated with Super M-MLV reverse transcriptase (BioTeke) to form the complementary DNA (cDNA) template. The final quantitative real-time polymerase chain reaction (RT-qPCR) reaction mixture contained 10 µL SYBR GREEN mastermix, 0.5 µL of each primer (PKM2, forward: 5′-CGCTGGATAACGCCTACAT-3′, backward: 5′-CCATTTTCCACCTCCGTC-3′; GAPDH, forward: 5′-ATGTTGCAACCGGGAAGGAA-3′, backward: 5′-AGGAAAAGCATCACCCGGAG-3′), 1 µL cDNA template, and 8 µL double-distilled water. The amplification

procedure included a denaturation step at 94° C for 10 minutes, followed by 40 cycles at 94 °C for 10 seconds, 60 °C for 20 seconds, and 72 °C for 30 seconds. The relative expression levels of PKM2 were calculated with the Data Assist Software version 3.0 (Applied Biosystems/Life Technologies). The $2^{-\triangle\triangle ct}$ method was used to estimate the expression levels of the gene of interest and of the GAPDH gene, which was used as the internal reference gene.

Immunohistochemical Detection

Immunohistochemical (IHC) detection was performed routinely. The paraffin sections were dewaxed, hydrated, and fixed prior to incubation with the primary antibody (Supplemental Table S1) at 4 °C overnight. The following day, the secondary antibody (Supplemental Table S1) was incubated with the sections at 37 °C for 30 minutes, which were further incubated with horseradish peroxidase-labeled avidin at 37 °C for 30 minutes prior to addition of diaminobenzidine. The slides were restained using hematoxylin and dehydrated. The determination of the IHC score was performed with an AperioScanScope GL system (Aperio Technologies) at ×100 magnification using the AperioImageScope software (Aperio Technologies). The percentage of positively stained cells was estimated as follows: The score of 0 to 4 was defined as low PKM2 expression, whereas the score of 4 to 7 was defined as high PKM2 expression.

Western Blot Assay

Total protein was extracted using the Total Protein Extraction Kit according to the manufacturer instructions (Wanleibio). The concentration levels of the protein samples were determined using the bicinchoninic acid (BCA) method. A total of 40 µg protein was separated in a 10% sodium dodecyl sulfate polyacrylamide gel and subsequently transferred onto a polyvinylidene difluoride membrane for incubation with skimmed milk powder solution for 1 hour. The membrane was further incubated with primary antibodies (Supplemental Table S1) at 4 °C overnight and with a secondary antibody (Supplemental Table S1) at 37 °C for 45 minutes. The protein blots were developed using Beyo ECL Plus reagent, and the images were captured using the corresponding gel imaging system. The relative expression levels of the proteins were calculated with the Gel-Pro-Analyzer (Media Cybernetics). The reference control groups included GAPDH as the internal reference protein.

Knockdown of PKM2

Pyruvate kinase M2-specific short hairpin RNA (shRNA) (5'-GTTCGGAGGTTTGATGAAATC-3') sequence and a matched nontargeting control (NC) sequence were obtained from Genechem Biotech (Shanghai). The shRNAs were inserted into the pRNA-H1.1 plasmid to form pRNA-H1.1-PKM2 and pRNA-H1.1-NC plasmids, which were used for knockdown of PKM2. The transfection of the shRNAs into the CNE2 and HNE1 cells was performed using Lipofectamine 2000. The transfection efficiency was determined following 24 hours, using RT-qPCR and Western blotting as described above (Supplemental Figure S1).

Cell Counting Kit 8 assay

Cell Counting Kit 8 (CCK-8) assays were performed to determine cell viability under different treatment conditions. Exponentially growing NPC cells were incubated in 96-well plates (3×10^3/well) for 72 hours (12 replicates for each group). Every 24 hours, the CCK-8 solution (10 µL) was added into 3 randomly selected wells and incubated at 37 °C for another 1 hour. Cell viability was measured by the optical density (OD) value at 450 nm using a microplate reader (ELX-800, BIOTEK).

Hoechst Staining

The morphological changes of the cell nuclei were determined using Hoechst staining. The NPC cells were cultured in 12-well plates (5×10^4/well) for 24 hours at 37 °C and subsequently incubated with 0.5 mL Hoechst for 5 minutes. The images were captured using a fluorescence microscope (IX53, Olympus) at ×400 magnification.

Transwell Assay

Cell invasive ability was assessed using a Transwell system covered with polycarbonate Transwell filters (Corning). The procedure was as follows: A total of 2×10^4 cells were transferred into the upper chamber with 0.2 mL serum-free Dulbecco modified Eagle medium (DMEM). The cells were incubated at 37 °C for 24 hours, and the percentage of cells penetrating across the membrane was estimated by Giemsa staining (Sigma-Aldrich). The stained cells were imaged under the microscope and their number was quantified.

Glucose Uptake Detection

Glucose uptake in NPC cells was determined using the ^{18}F-fluorodeoxyglucose (^{18}F-FDG) uptake assay as follows: The cells were cultured in 12-well plates (2×10^5/well) with 500 µL of DMEM containing 4 µCi/mL ^{18}F-FDG at 37 °C for 1 hour. Subsequently, the pellets were washed with ice-cold phosphate buffered saline and lysed using 500 µL 0.1 M NaOH. The radioactivity of the total cell lysates was assayed using a PerkinElmer Automatic Wizard2 Gamma Counter.

Detection of ATP Production

The relative content of ATP in NPC cells was determined using the ATP bioluminescent somatic cell assay kit (Sigma) according to the manufacturer instructions. Briefly, the cells were cultured in 24-well plates (2×10^5/well) for 24 hours and lysed. The lysates were collected and subjected to a luminescence reader for the determination of the luminescence
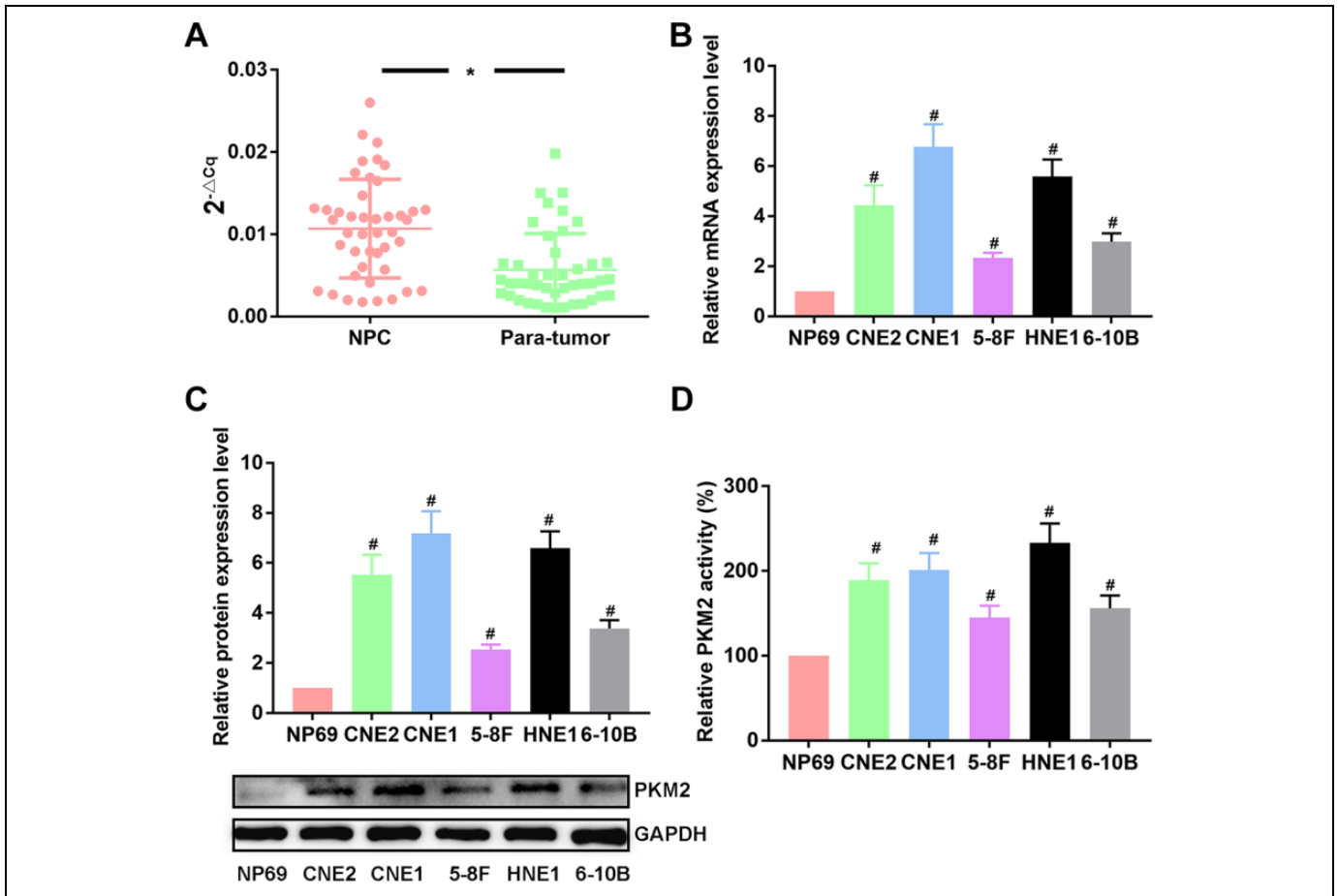
Figure 1. Expression and activity of PKM2 are abnormally high in NPC samples and NPC cell lines. The expression level of PKM2 was determined in 44 pairs of NPC samples and corresponding paratumor samples with RT-qPCR (A). Then the results were further verified with NPC cell lines in reference to human nasopharyngeal epithelial cell line NP69 with RT-qPCR (B), Western blotting assays (C), and ELISA kit (D). "*" represents statistically significant difference from NPC, $P < .05$. "#" represents statistically significant difference from NP69 cell line, $P < .05$. ELISA indicates enzyme-linked immunosorbent assay; NPC, nasopharyngeal carcinoma; PKM2, pyruvate kinase M2; RT-qPCR, quantitative real-time polymerase chain reaction.

intensity. The results were represented as the relative intracellular ATP level compared with that of the parental cells.

Glycolytic Pathway Activity Detection

The activity of the glycolytic pathway was determined by quantifying the levels of the different products of glycolysis. The production of pyruvic acid (cat. No. A081, Nanjing Jiancheng Bioengineering Institute, Nanjing, China) and lactate (cat. No. A019-2, Nanjing Jiancheng Bioengineering Institute, Nanjing, China) was measured using corresponding kits according to manufacturer instructions: Briefly, the total protein was extracted from the sample and the protein concentration was determined using BCA method. Afterward, the level of product was measured by mixing solutions from kits with the sample and calculated in reference to protein concentration. The production of fructose-6-phosphate (cat. No. K689, BioVision) and malate (cat. No. K637, BioVision) was measured using corresponding kits according to manufacturer

instructions: Briefly, cells ($1 \times 10^5/\mu L$) were incubated with solutions in the kits and the OD values at 450 nm were detected. The levels of products were calculated using OD_{450} values in reference to a standard curve for product concentration.

Statistical Analysis

Continuous data are expressed as mean $\pm$ standard deviation ($n = 3$), and categorical data are presented as the number of frequency distribution. The association between PKM2 levels and different clinicopathological indices was analyzed using the Wilcoxon rank-sum test. The differences between groups were analyzed using one-way analysis of variance followed by multiple comparisons using the Tukey method. Statistical analysis and graph plotting were conducted using Graphpad Prism version 6.0 (GraphPad Software, Inc). A 2-tailed $P < .05$ was considered to indicate a statistically significant difference.

Results

Levels of PKM2 Are Upregulated in NPC Clinical Samples and NPC Cell Lines

The expression levels of PKM2 in NPC specimens were detected with RT-qPCR assays and compared with those noted in the paratumor tissues. The average relative expression status was significantly higher in NPC tissues than that noted in the corresponding paratumor tissues (Figure 1A, $P < .05$). The abnormally high expression level of PKM2 in NPC was further verified using NPC cell lines. The relative expression levels of PKM2 were higher in the NPC cells compared with those noted in the human nasopharyngeal epithelial cells ($P < .05$; Figure 1B and C). CNE2 and HNE1 cells exhibited the highest expression levels of PKM2. Corresponding to the changes in PKM2 messenger RNA and protein levels, the activity of PKM2 in CNE1, CNE2, and HNE1 was higher than that in other cell lines (Figure 1D).

Levels of PKM2 Are Associated With the Growth and Metastatic Activity of NPC Cells

Expression levels of PKM2 were further detected in samples derived from 44 individuals using IHC assays and scored accordingly (Supplemental Figure S2). PKM2-positive cells were characterized by the presence of yellowish-brown particles. Based on the scores, the association between PKM2 expression status and clinicopathological characteristics of patients with NPC was analyzed. The analysis indicated that the parameters age and gender exhibited no influence on the expression levels of PKM2, while increased expression levels of PKM2 were associated with advanced tumor size, lymph node metastasis, distant metastasis, and tumor–node–metastasis stage ($P < .05$; Table 1), indicating the potential of PKM2 as a NPC prognostic marker.

Knockdown of PKM2 Inhibits Cell Viability and Invasion While Inducing Apoptosis in NPC Cells

To explore the role of PKM2 in NPC cell proliferation and mobility, its expression was inhibited with shRNA in CNE2 and HNE1 cells (relatively high PKM2 level). Based on the results of the CCK-8 assay, the viability of NPC cells was suppressed in the PKM2-knockdown groups compared with that noted in the NC groups (Figure 2A and B). Significant differences were detected following 48 hours of incubation of the PKM2-knockdown cells ($P < .05$). The effects of PKM2 knockdown on the invasive activity of NPC cells were also evaluated. The average number of the cells penetrating the membrane (28.8 ± 2.4 for CNE2 cells and 24.2 ± 1.5 for HNE1 cells) was significantly lower than those (60.2 ± 6.6 for CNE2 cells and 37.6 ± 5.7 for HNE1 cells) in the NC groups ($P < .05$; Figure 2C and D). In contrast to these observations, induction of apoptosis was noted in NPC cells. The number of bright blue cells (under apoptosis) was higher in

Table 1. Relation Between PKM2 Expression Status and Clinicopathological Characteristics.

Parameter	PKM2 level		P value
	High (33)	Low (11)	
Gender			
Male	16	4	
Female	17	7	.728
Age			
<60	14	6	
≥60	19	5	.509
Histological type			
DNKC	21	9	
UDC	12	2	.457
Tumor size			
T1-T2	5	7	
T3-T4	18	4	.026[a]
Lymph node metastasis			
M0	7	8	
M1	16	3	.030[a]
Clinical stage			
I-II	3	7	
III-IV	20	4	.005[a]

Abbreviations: DNKC, nonkeratinizing carcinoma; PKM2, pyruvate kinase M2; UDC, undifferentiated carcinoma.
[a]$P < 0.05$ vs. High.

PKM2-knockdown cells compared with that noted in parental NPC cells (Figure 2E and F). Taken together, the results suggested the key function of PKM2 in maintaining the growth and metastasis of NPC cells.

Knockdown of PKM2 Inhibits the Warburg Effect in NPC Cells

Following knockdown of PKM2, the uptake of glucose was decreased by 27% and 25% in CNE2 and HNE1, respectively ($P < .05$; Figure 3A and B). Moreover, the production of ATP was also dramatically induced corresponding to the decreased glucose uptake in NPC cells (Figure 3C and D), implying the transition of glucose metabolism from glycolysis to mitochondrial respiration. In addition, the inhibition of PKM2 suppressed the production of pyruvic acid, lactate, citrate, and malate in NPC cells, confirming the inhibition of glycolysis ($P < .05$; Figure 4A and D). However, the production of fructose-6-phosphate was not significantly influenced by the inhibition of PKM2 (Figure 4E). These observations confirmed the inhibitory effect of PKM2 knockdown on the Warburg effect in NPC cells.

Knockdown of PKM2 Inhibits the Expression Levels of the Glucose Uptake- and Glycolysis-Associated Kinase in NPC Cells

Further analysis of the changes in the expression levels of the kinase enzyme associated with glucose uptake or glycolysis
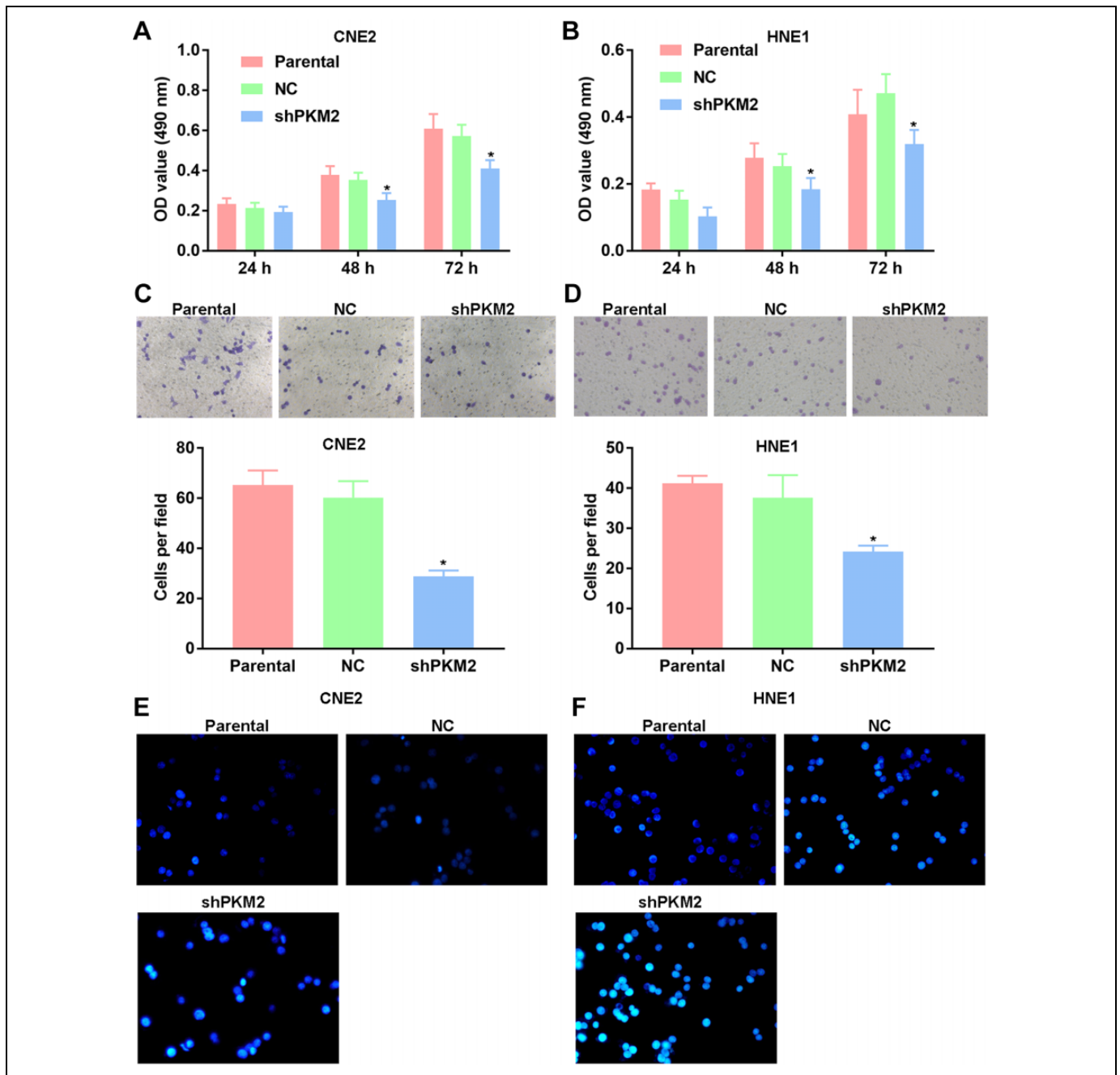
Figure 2. PKM2 inhibition reduces viability and invasion, while induces apoptosis in NPC cell lines. The viability (A and B), invasion (C and D), and morphological changes in nuclei (E and F) in NPC cells transfected with PKM2 shRNA were determined using CCK-8, transwell assay, and Hoechst staining respectively. "*" represents statistically significant difference from NC group, $P < 0.05$.

metabolism was performed by Western blot assays. Knockdown of PKM2 led to the downregulation of glucose transporter 1 (GLUT1) which was the major glucose transporter identified in the cell model used compared with the NC groups ($P < .05$). Moreover, the expression levels of hexokinase 2 (HK2), which is the key enzyme of glycolysis, were also suppressed by PKM2 inhibition (Figure 5A and B). However, the expression levels of 6-phosphofructokinase 1 were not influenced by PKM2 knockdown, partially explaining the

production pattern of fructose-6-phosphate in PKM2-knockdown NPC cells (Figure 5A and B). The results further confirmed the impaired glucose uptake and glycolysis in NPC cells with dysfunctional PKM2.

Discussion

Glycolysis under aerobic conditions has been recognized as an essential component contributing to the progression of
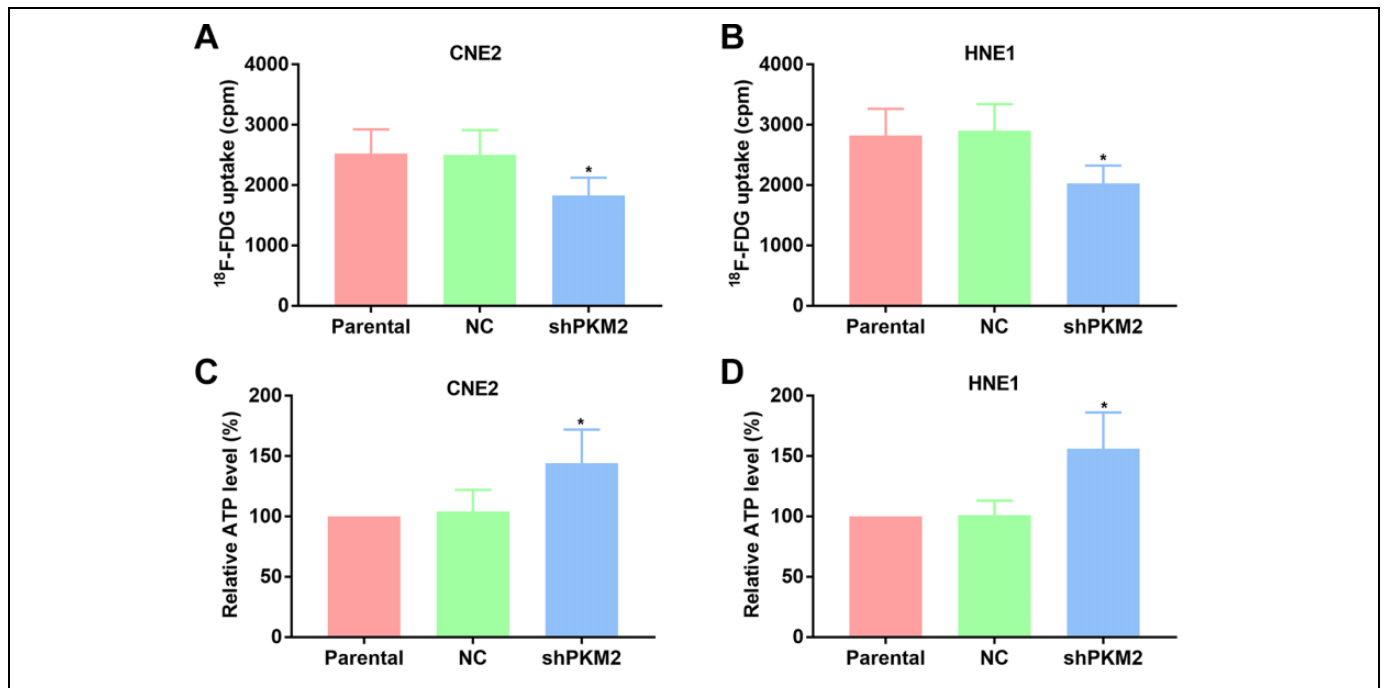
Figure 3. Inhibition of PKM2 suppresses glucose uptake, while increases ATP production in NPC cell lines. The glucose uptake (A and B) and relative ATP production (C and D) in NPC cell lines transfected with PKM2 shRNA were measured using ^{18}F-FDG uptake assay and ATP bioluminescent somatic cell assay kit. The 2 assays were performed independently to avoid the influence on the ATP production by ^{18}F-FDG. "*" represents statistically significant difference from NC group, $P < .05$. ^{18}F-FDG indicates ^{18}F-fluorodeoxyglucose; NPC, nasopharyngeal carcinoma; PKM2, pyruvate kinase M2; shRNA, short hairpin RNA.
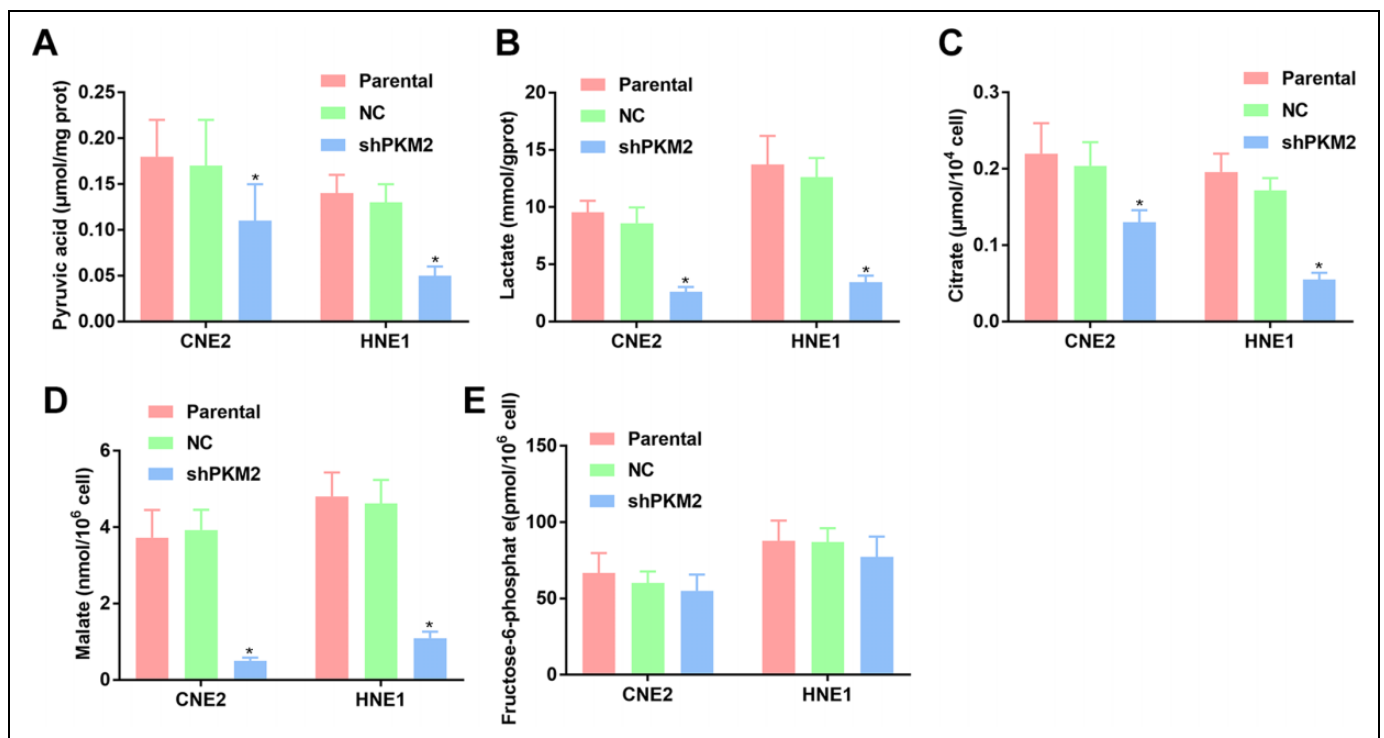
Figure 4. Inhibition of PKM2 inhibits production of metabolism in glycolytic metabolism. The production of pyruvic acid (A), lactate (B), citrate (C), malate (D), and fructose-6-phosphate (E) was detected with corresponding detective kits. "*" represents statistically significant difference from NC group, $P < .05$. NC indicates nontargeting control; PKM2, PKM2, pyruvate kinase M2.
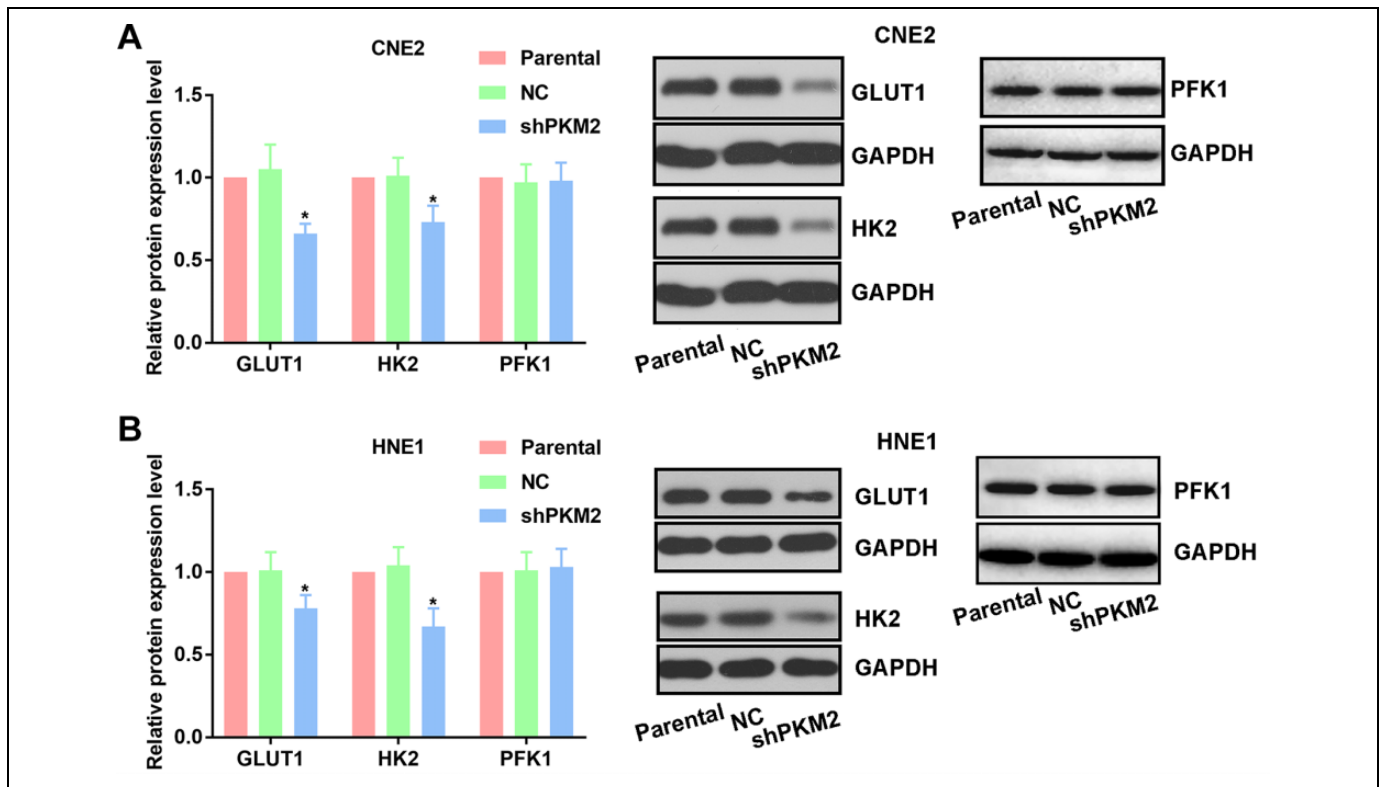
Figure 5. Inhibition of PKM2 downregulated members involved in glucose uptake and glycolytic metabolism. The expression levels of GLUT1, HK2, and PFK1 were detected with Western blotting assays (A and B). "*" represents statistically significant difference from NC group, $P < .05$.

malignancies, which is defined as the "Warburg effect."[19] In the majority of cancer types, overexpression of glycolytic genes plays a central role in the establishment of the Warburg effect.[20] Therefore, appropriate inhibition of glycolytic genes has been proposed as a promising strategy to suppress the Warburg effect and control cancer development. Pyruvate kinase M2 is closely associated with glucose metabolism and is highly expressed in different cancer types.[21] The inhibition of PKM2 has been shown to inhibit progression of different cancer types through multiple mechanisms of action. For example, inhibition of PKM2 suppresses aerobic glycolysis, decreases lactate production, and reduces cell proliferation and migration in colorectal cancer cells.[20] Moreover, knockdown of PKM2 inhibits tumor survival and invasion in osteosarcoma.[18] Previous studies have provided ample evidence regarding the use of PKM2 inhibition as an alternative strategy for controlling cancer development. Therefore, the current study performed a series of assays and analyses to demonstrate the role of PKM2 in the progression of NPC. Although several studies have been previously reported with regard to the function of PKM2 in oncogenesis, its role in NPC has not been previously explored.

The expression status of PKM2 was initially assessed in NPC specimens, and its association with the patient clinicopathological characteristics was analyzed. The RT-qPCR analysis revealed that PKM2 levels were significantly upregulated in NPC tissues compared with the corresponding levels noted in adjacent normal tissues. This finding was verified in NPC cell lines. It was found that the relative expression levels of PKM2 in NPC cell lines was considerably higher than that noted in nasopharyngeal epithelial cells, confirming the elevated levels of PKM2 with the onset of NPC. The expression levels of PKM2 in NPC samples were also assessed using IHC, and the results were compared with the patient clinicopathological characteristics. The analysis indicated that PKM2 levels were positively associated with tumor growth and metastasis. Expression of PKM2 was closely associated with the development of NPC, notably with regard to the growth and metastatic activity of the cancer cells. To support these findings, the results derived from the clinical samples were further validated in cell line models.

The expression of PKM2 was inhibited with shRNA in 2 NPC cell lines. The results indicated that the expression of PKM2 was important for the proliferation and invasion of NPC cells. Knockdown of PKM2 decreased the OD_{450} value, induced apoptosis, and reduced the membrane-penetrating cell number. It is widely accepted that tumor cells require high levels of ATP that are provided by extensive glucose metabolism.[13,22-24] Pyruvate kinase catalyzes the last step in the glycolytic cascade and consequently the activity of PKM2 controls the rate of glycolysis.[25] Therefore, the effect of PKM2 knockdown on glucose metabolism in NPC cells was investigated. The results indicated that inhibition of PKM2 led to repressed glucose uptake and ATP production. Inhibition of PKM2

contributed to decreased production of pyruvic acid, lactate, citrate, and malate in NPC cells, indicating impaired glycolytic process. The expression levels of the kinase enzymes involved in glucose uptake and glycolysis were also downregulated by PKM2 inhibition: the inhibited activity of PKM2 reduced the production of pyruvic acid, which in return led to the accumulation of intermediate products of glycolysis and inhibited the activity of other enzymes, such as HK2 and GLUT1. These results demonstrated that in PKM2-suppressed NPC cells glucose metabolism was mediated by mitochondrial respiration and not by aerobic glycolysis, which substantially increased the production of ATP with similar energy sources, that is, glucose, even with the reduced production of pyruvate, citric acid, and malate. The activity of PKM2 is adjusted based on specific cell requirements for proliferation, growth, and survival. This is achieved by transitioning between catabolic and anabolic pathways based on cell needs.[26] This characteristic benefits tumor cell survival since high levels of PKM2 produce sufficient ATP and carbon unit production that can maintain the malignant phenotypes of tumor cells. Sun *et al* further demonstrated that the synthesis of lipids in lung carcinoma was inhibited following inhibition of PKM2, which further supported this theory.[27] However, the downstream effectors of PKM2 are multiple and other carcinogenesis-related factors, such as matrix metalloproteinases and vascular endothelial growth factor, can also respond to the activity changes of PKM2.[28-31] Therefore, future comprehensive exploration with the aid of omic technology is required for understanding the detailed function of PKM2 in the progression of NPC and of other cancer types.

In conclusion, the current study described the key role of PKM2 in the abnormal metabolism of glucose in NPC. The expression of this enzyme was upregulated in NPC tissues and inhibition of PKM suppressed the Warburg effect by decreasing glucose uptake and aerobic glycolysis in NPC cells. The changes noted in glucose metabolism led to the suppressed proliferation and metastatic activity of NPC cells. Nevertheless, the current study failed to provide sufficient information regarding the downstream effectors of PKM2 in promoting NPC. Therefore, additional work should be performed in future studies to facilitate the application of PKM2-based strategies in inhibiting NPC progression.

Declaration of Conflicting Interests

The author(s) declared no potential conflicts of interest with respect to the research, authorship, and/or publication of this article.

Ethics Statement

The collection of relating data was approved by the ethic committee of The First People's Hospital of Wenling (approve file: 20160034) and all the works were undertaken following the provisions of the Declaration of Helsinki.

Funding

The author(s) received no financial support for the research, authorship, and/or publication of this article.

ORCID iD

Renjie Su https://orcid.org/0000-0002-9857-3223

Supplemental Material

Supplemental material for this article is available online.

References

1. Chen YP, Chan ATC, Le QT, Blanchard P, Sun Y, Ma J. Nasopharyngeal carcinoma. *Lancet*. 2019;394(10192):64-80.
2. Siegel RL, Miller KD, Jemal A. Cancer statistics, 2016. *CA*. 2016; 66(1):7-30.
3. Lam WKJ, Chan JYK. Recent advances in the management of nasopharyngeal carcinoma. *F1000Res*. 2018;7:F1000 Faculty Rev-1829.
4. Andersson Anvret M, Forsby N, Klein G, Henle W. Relationship between the Epstein-Barr virus and undifferentiated nasopharyngeal carcinoma: correlated nucleic acid hybridization and histopathological examination. *Int J Cancer*. 1977;20(4):486-494.
5. Lin DC, Meng X, Hazawa M, et al. The genomic landscape of nasopharyngeal carcinoma. *Nat Genet*. 2014;46(8):866-871.
6. Schwartz L, T Supuran C, O Alfarouk K. The Warburg effect and the hallmarks of cancer. *Anti-Cancer Agent Me*. 2017;17(2): 164-170.
7. Warburg O. On the origin of cancer cells. *Science*. 1956; 123(3191):309-314.
8. Su Y, Yu QH, Wang XY, et al. JMJD2A promotes the Warburg effect and nasopharyngeal carcinoma progression by transactivating LDHA expression. *BMC Cancer*. 2017;17(1):477.
9. Zhao Y, Yang L, He J, Yang H. STYK1 promotes Warburg effect through PI3K/AKT signaling and predicts a poor prognosis in nasopharyngeal carcinoma. *Tumor Biol*. 2017;39(7): 1010428317711644.
10. Liu Y, He X, Chen Y, Cao D. Long non-coding RNA LINC00504 regulates the Warburg effect in ovarian cancer through inhibition of miR-1244. *Mol Cell Biochem*. 2020;464(1-2):39-50.
11. Yang X, Zhao H, Yang J, et al. MiR-150-5p regulates melanoma proliferation, invasion and metastasis via SIX1-mediated Warburg effect. *Biochem Bioph Re Commun*. 2019;515(1):85-91.
12. Christofk HR, Vander Heiden MG, Harris MH, et al. The M2 splice isoform of pyruvate kinase is important for cancer metabolism and tumour growth. *Nature*. 2008;452(7184): 230-233.
13. Christofk HR, Vander Heiden MG, Wu N, Asara JM, Cantley LC. Pyruvate kinase M2 is a phosphotyrosine-binding protein. *Nature*. 2008;452(7184):181-186.
14. Anastasiou D, Poulogiannis G, Asara JM, et al. Inhibition of pyruvate kinase M2 by reactive oxygen species contributes to cellular antioxidant responses. *Science*. 2011;334(6060): 1278-1283.
15. Eigenbrodt E, Reinacher M, Scheefers-Borchel U, Scheefers H, Friis R. Double role for pyruvate kinase type M2 in the expansion of phosphometabolite pools found in tumor cells. *Critic Rev Oncogene*. 1992;3(1-2):91-115.

16. Lunt SY, Muralidhar V, Hosios AM, et al. Pyruvate kinase isoform expression alters nucleotide synthesis to impact cell proliferation. *Mol Cell*. 2015;57(1):95-107.

17. Sun H, Zhu A, Zhang L, Zhang J, Zhong Z, Wang F. Knockdown of PKM2 suppresses tumor growth and invasion in lung adenocarcinoma. *Int J Mol Sci*. 2015;16(10):24574-24587.

18. Yuan Q, Yu H, Chen J, Song X, Sun L. Knockdown of pyruvate kinase type M2 suppresses tumor survival and invasion in osteosarcoma cells both in vitro and in vivo. *Exp Cell Res*. 2018;362(1):209-216.

19. Xu XD, Shao SX, Jiang HP, et al. Warburg effect or reverse Warburg effect? A review of cancer metabolism. *Oncol Res Treat*. 2015;38(3):117-122.

20. Zhou CF, Li XB, Sun H, et al. Pyruvate kinase type M2 is upregulated in colorectal cancer and promotes proliferation and migration of colon cancer cells. *IUBMB life*. 2012;64(9):775-782.

21. Dayton TL, Jacks T, Vander Heiden MG. PKM2, cancer metabolism, and the road ahead. *EMBO Rep*. 2016;17(12):1721-1730.

22. Mazurek S, Boschek CB, Hugo F, Eigenbrodt E. Pyruvate kinase type M2 and its role in tumor growth and spreading. *Semin Cancer Biol*. 2005;15(4):300-308.

23. Zwerschke W, Jansen-Dürr P. Cell transformation by the E7 oncoprotein of human papillomavirus type 16: interactions with nuclear and cytoplasmic target proteins. *Adv Cancer Res*. 1999;78:1-29. Elsevier.

24. Hitosugi T, Kang S, Vander Heiden MG, et al. Tyrosine phosphorylation inhibits PKM2 to promote the Warburg effect and tumor growth. *Sci Signal*. 2009;2(97):ra73-ra73.

25. Liu VM, Vander Heiden MG. The role of pyruvate kinase M2 in cancer metabolism. *Brain Pathol*. 2015;25(6):781-783.

26. Spoden GA, Rostek U, Lechner S, Mitterberger M, Mazurek S, Zwerschke W. Pyruvate kinase isoenzyme M2 is a glycolytic sensor differentially regulating cell proliferation, cell size and apoptotic cell death dependent on glucose supply. *Exp Cell Res*. 2009;315(16):2765-2774.

27. Beckner ME, FellowsMayle W, Zhang Z, et al. Identification of ATP citrate lyase as a positive regulator of glycolytic function in glioblastomas. *Int J Cancer*. 2010;126(10):2282-2295.

28. Kim YM, Jang JW, Lee OH, et al. Endostatin inhibits endothelial and tumor cellular invasion by blocking the activation and catalytic activity of matrix metalloproteinase 2. *Cancer Res*. 2000;60(19):5410-5413.

29. Yang W, Xia Y, Hawke D, et al. PKM2 phosphorylates histone H3 and promotes gene transcription and tumorigenesis. *Cell*. 2012;150(4):685-696.

30. Yeluri S, Madhok B, Prasad KR, Quirke P, Jayne DG. Cancer's craving for sugar: an opportunity for clinical exploitation. *J Cancer Res Clin*. 2009;135(7):867.

31. Gillies RJ, Robey I, Gatenby RA. Causes and consequences of increased glucose metabolism of cancers. *J Nucl Med*. 2008;49(2):24S.